Available online at www.sciencedirect.com
SCIENCE DIRECT
Journal of Photochemistry and Photobiology A: Chemistry 176 (2005) 199–207
Journal of Photochemistry and Photobiology A:Chemistry
www.elsevier.com/locate/jphotochem

Experimental product study of the OH-initiated oxidation of *m*-xylene

Jun Zhao [a], Renyi Zhang [a,*], Kentaro Misawa [b], Kazuhiko Shibuya [b]

[a] *Department of Atmospheric Sciences, Texas A&M University, 1204 Eller O&M Building, 3150 TAMU, College Station, TX 77843, USA*
[b] *Department of Chemistry, Graduate School of Science and Engineering, Tokyo Institute of Technology, 2-12-1-H3-57, Ohokayama, Meguro-ku, Tokyo 152-8551, Japan*

Received 23 May 2005; received in revised form 14 July 2005; accepted 17 July 2005
Available online 13 September 2005

Abstract

We performed laboratory studies to investigate the OH-initiated oxidation of *m*-xylene using a fast flow reactor coupled to ion drift-chemical ionization mass spectrometry (ID-CIMS). Seven products consisting of ring-retaining and ring-opening components have been identified and quantified. Three products, methylglyoxal, 4-oxo-2-pentenal and 2-methyl-4-oxo-2-butenal, and dimethylphenols exhibited a dependence of the formation yields on the O_2 and NO concentration. We reported for the first time the yields (%) of three other products, 2-methyl-4-oxo-2-penetal (4.89 ± 0.52), diunsaturated dicarbonyls (2-methyl-6-oxo-2,4-heptadienal and 4-methyl-6-oxo-2,4-heptadienal, 7.82 ± 1.0), and epoxy carbonyls (2,4-dimethyl-2,3-epoxy-6-oxo-4-hexenal, 2,6-dimethyl-2,3-epoxy-6-oxo-4-hexenal, and 3,5-dimethyl-2-hydroxyl-3,4-epoxy-5-hexenal, 2.18 ± 0.20). *m*-Tolualdehyde, with a yield of 6.42 ± 0.89, is consistent with previous studies. The yield of methylglyoxal (15.1 ± 4.2) is consistent with its co-products, but lower than the literature values. The dependence of product distributions on O_2 and NO concentration was discussed. The mechanism leading to the formation of the products was proposed.

Keywords: Aromatic oxidation; Products; Air chemistry

1. Introduction

Aromatic hydrocarbons constitute an important fraction (∼20%) of total volatile organic compounds (VOCs) in the urban atmosphere and play a major role in urban air pollution [1–3]. In addition to their significant contributions to photochemical ozone production, oxidation of aromatic hydrocarbons leads to formation of non-volatile and semi-volatile organic compounds, which are important precursors of secondary organic aerosol (SOA) [4,5]. Recently evidence has been found for the formation of potentially toxic and mutagenic epoxide products from photo-oxidation of aromatic hydrocarbons [6]. Also, carboxylic acids, which enhance formation of new particles in the atmosphere [7], are produced from aromatic hydrocarbon oxidation.

Xylenes (*m*-, *p*-, and *o*-xylene) are important constitutions of aromatic hydrocarbons and are highly reactive with respect to ozone formation [8]. In the atmosphere, the dominant loss process for xylenes is the gas-phase reaction with the hydroxyl radical OH. Their reaction rates with OH radicals are on the order of 10^{-11} cm^3 molecule^{-1} s^{-1} [9,10], nearly four times higher than that of toluene [1]. The OH-initiated reaction results in minor H-abstraction from one methyl group to form a methylbenzyl radical (about 10%) and major OH addition to the aromatic ring to form a dimethylhydroxycyclohexadienyl radical (about 90%) [1–3]. In the presence of O_2 and NO, the subsequent reactions of the methylbenzyl radicals lead to the formation of tolualdehydes and methylbenzyl nitrates. The dimethylhydroxycyclohexadienyl radicals (the OH–xylene adduct) formed from the addition pathway react dominantly with O_2 in the atmosphere, although its reaction rate constant with NO_2 is about 10^5 higher than with O_2 at room temperature [10–12]. Under atmospheric conditions, the OH–xylene adduct reacts with O_2 either by O_2 addition to form primary peroxy radicals or by H-abstraction to yield phenolic compounds (e.g. dimethylphenols), or by H-abstraction to form aromatic oxide/oxepin (Scheme 1).

* Corresponding author. Tel.: +1 979 845 7656; fax: +1 979 862 4466.
E-mail address: zhang@ariel.met.tamu.edu (R. Zhang).

1010-6030/$ – see front matter © 2005 Elsevier B.V. All rights reserved.
doi:10.1016/j.jphotochem.2005.07.013

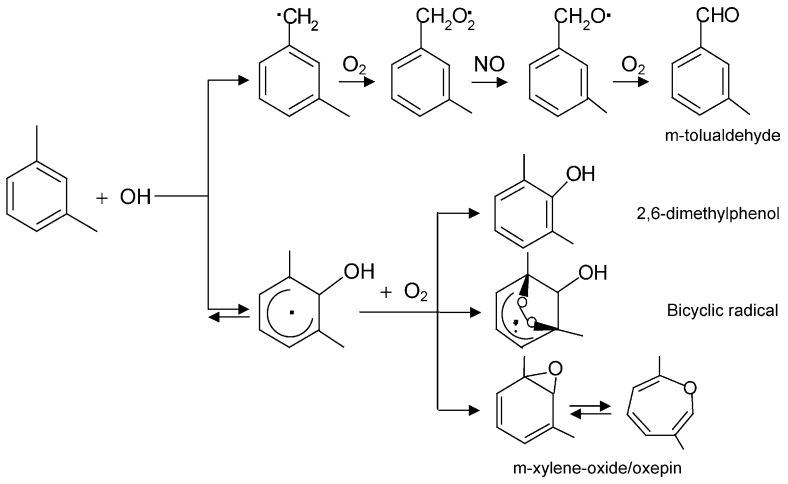

Scheme 1. Mechanistic diagram for the OH-initiated oxidation of *m*-xylene.

The fate of the primary peroxy radicals is governed by competition between reaction with NO to form alkoxy radicals and intramolecular cyclization to form bicyclic radicals. Theoretical studies have shown that, instead of reaction with NO, the primary peroxy radicals from OH-initiated oxidation of toluene cyclize, forming bicyclic radicals [13]. In the presence of NO, subsequent reactions of bicyclic radicals resulting from the OH-initiated oxidation of the xylenes lead to multi-functional organic compounds such as glyoxal, methylglyoxal, epoxides, and unsaturated carbonyl compounds. The aromatic oxide/oxepin channel leads to the formation of unsaturated dicarbonyls, although it remains uncertain.

Although numerous experiments have been carried out to study the products from OH-initiated xylenes oxidation [14–17], few are able to quantify the products and the quantified products account for less than 70% of the carbon balance for the individual xylene. For example, Smith et al. [14] reported the product distribution and obtained a total carbon yield of 41 and 65% for the measured products from *m*-xylene and *p*-xylene, respectively. Volkamer et al. [15] found experimental evidence for the bicyclic pathway from the oxidation of selected aromatic hydrocarbons and presented a molar yield of 40% for glyoxal from OH-initiated oxidation of *p*-xylene, in good agreement with Smith et al. Bethel et al. [16] studied the effect of NO_2 concentration on the OH–*p*-xylene reaction and found the dependency of product yields on NO_2 concentrations.

In this study, we employed a recently developed ion drift-chemical ionization mass spectrometry to identify and quantify ring-retaining (e.g. *m*-tolualdehyde and dimethylphenols) and ring-opening (e.g. methylglyoxal, unsaturated dicarbonyls, diunsaturated dicarbonyls, and epoxy carbonyls) products from OH-initiated oxidation of *m*-xylene in the present of O_2 and NO. The oxidation mechanisms for OH-initiated *m*-xylene oxidation were then proposed.

2. Experimental

The experiments were performed using a fast flow reactor in conjunction with ion drift–chemical ionization mass spectrometry detection. Detailed description of ID-CIMS technique can be found in a recent publication [18]. Only the aspects relevant to the present study are described in this work. Briefly, the ID-CIMS system consisted of three sections: (1) a fast flow reactor where gas-phase reaction occurred, (2) an ion drift tube where the reagent ions were produced and the proton/electron transfer reactions took place, and (3) ion detection system where the reagent and product ions were analyzed. The flow reactor was constructed from precision-bore Pyrex tubing of 2.0 cm i.d. and 75 cm in length. All surfaces exposed to the radicals were coated with halocarbon wax to reduce wall loss [19]. A flow of nitrogen carrier gas ($\sim$30 L min^{-1}) was introduced into the flow reactor through an entrance port in the sidearm of the flow reactor (Fig. 1). A high-capacity (700 L min^{-1}) oil-free vacuum pump was used to evacuate the flow reactor through an exit port in the downstream end of the reactor and the majority of the flow was directed through this port. Only a small frac-

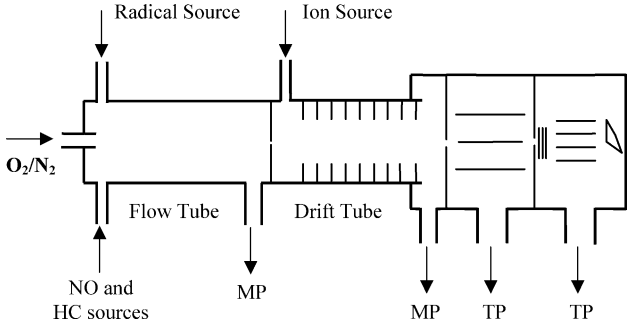

Fig. 1. Schematic diagram of the fast flow reactor coupled to an ion-drift chemical ionization mass spectrometry (ID-CIMS). MP represents the mechanical pump and TP for the turbo molecular pump.

tion (about 1%) of the flow was extracted into the drift tube through a small orifice (1 mm). The pressure in the flow reactor was monitored by a capacitance manometer (1000 Torr full scale) in the downstream end of the flow reactor and was regulated at about 100 Torr. All experiments were performed at 298 ± 2 K. Typical flow velocity in the flow reactor ranged from 800 to 1500 cm s^{-1}. All the gas flows were monitored with calibrated mass flow meters (Millipore Tylan 260 Series). Commercially available *m*-xylene (Alfa Aesar, 99%) was used as received without further purification. A 0.5% *m*-xylene/He mixture was prepared volumetrically in a 2 L glass bulb. The *m*-xylene mixture along with a small carrier flow of N_2 was then introduced into the flow reactor using a 10 sccm flow meter. O_2 (about 2–20% of the total flow) was also added into the flow reactor. NO was introduced through an activated carbon trap to remove impurities (e.g. NO_2) before being added to the reactor.

The ID-CIMS was capable of detecting and quantifying a species using either negative or positive reagent ion [18]. The OH–*m*-xylene reaction occurred in the flow reactor. The hydroxyl radical OH was generated by microwave discharge according to the reaction [20]

$$H + NO_2 \rightarrow OH + NO \quad (1)$$

Hydrogen atoms were produced by flowing a small amount of 3% H_2/He mixture through a microware discharge followed by adding an excess of a 1% NO_2/He mixture downstream. The generated OH radicals were then merged into the flow reactor. OH radicals were detected and optimized with negative reagent ion SF_6^-. SF_6^- ions were generated by adding a small amount of SF_6 to a nitrogen carrier flow (about 500 sccm), which then passed through the corona discharge. A negative voltage (−5 kV) was applied to the electrode of the discharge. SF_6^- and product ions were then guided by a negative electric field (about 2.0 V cm^{-1}) through the drift tube. The ion–molecule reaction between OH and SF_6^- occurred in the drift tube region [21],

$$OH + SF_6^- \rightarrow SF_6 + OH^- \quad (2)$$

The OH concentration was estimated using the procedures similar to those in our previous studies [22].

The products were monitored and quantified using hydronium ion (H_3O^+) as the reagent ion. H_3O^+ ions were generated by leaking a small amount of water vapor from a bubbler containing deionized water into the nitrogen flow, which then passed through the corona discharge. The amount of water vapor was controlled by adjusting the flow through the bubbler. For the proton transfer reaction,

$$R + H_3O^+ \rightarrow H_2O + RH^+ \quad (3)$$

only a small fraction of reagent ions H_3O^+ were converted into product ions RH^+, which were then detected by the mass spectrometry. The abundant of the species R can be quantified from the equation,

$$[R] = \frac{S(RH^+)}{k_3 \times S(H_3O^+) \times dt} \quad (4)$$

where d*t* is ion-drift reaction time on the order of 10^{-5} s and $S(RH^+)$ and $S(H_3O^+)$ are the intensities of RH^+ and H_3O^+, respectively. This method allows product yield measurements without the necessity of calibration, provided that the proton transfer reaction rate constant k_3 is available. We have previously demonstrated the advantage in applying ID-CIMS to quantify product yields of OH–isoprene oxidation reaction [23]. The product yield of the OH–*m*-xylene oxidation is derived according to Eq. (4) by assuming $S(H_3O^+) \approx S(H_3O^+)_0$ during the experiment,

$$Y(\%) = \frac{\Delta[prod]}{\Delta[mxy]} = \frac{k_{mxy}}{k_{prod}} \times \frac{\Delta S_{prod}}{\Delta S_{mxy}} \quad (5)$$

where $S(H_3O^+)_0$ is the intensity of H_3O^+ ions in the absence of the reactants. Δ[prod]/Δ[mxy] is the ratio of the product formed to *m*-xylene consumed. $\Delta S_{prod}/\Delta S_{mxy}$ is the ratio of the intensity of the protonated product species generated to the protonated *m*-xylene reacted. k_{prod} and k_{mxy} are the ion–molecule rate constants for the proton transfer reactions between the product species and H_3O^+ and between *m*-xylene and H_3O^+, respectively. By successively varying the *m*-xylene concentration, we determined the product yields according to Eq. (5). The ion–molecule reaction rates between H_3O^+ and the product species were determined using the average-dipole orientation (ADO) theory, which has been validated for accuracy for a series of hydrocarbons and oxygenated organic species [24]. Calibration showed an excellent agreement between the *m*-xylene concentrations estimated from the known volumetric mixing ratio of the gas standard in the flow reactor and that measured by the ID-CIMS method (within 10%).

3. Results

A series of experiments were carried out to investigate the primary products from the OH-initiated oxidation of *m*-xylene under the conditions summarized in Table 1. A total flow of ∼30 L min^{-1} was introduced to ensure the experiments under turbulent flow conditions (Reynolds number $Re \geq 2000$). Prior to each measurement, OH was initially monitored and optimized with the negative ion mode. The initial OH concentration was estimated to be in the range of (20–70) ppbv. In order to minimize possible secondary reactions between the OH–*m*-xylene adduct and NO_2, the NO_2 concentration was also monitored with the negative ion mode and kept at a low level. Typical NO_2 concentration was about 20–45 ppbv. *m*-Xylene was introduced into the flow rector and was allowed to react with OH along the flow reactor with a typical reaction time of ∼0.05 s. After entering the drift tube, *m*-xylene and the oxidation products underwent pro-

Table 1
Summary of the experimental conditions[a]

Experiment no.	*m*-Xylene (ppm)	OH (ppb)	O_2 (%)	NO (ppm)	NO_2 (ppb)
Condition I					
1	0.31–1.23	70.0	2	0.33	20.7
2	0.31–1.43	41.8	2	0.33	36.5
3	0.36–1.34	52.2	2	0.39	40.7
4	0.27–1.32	46.3	2	0.29	32.6
5	0.29–1.39	21.2	2	0.31	34.3
6	0.30–1.38	27.4	2	0.31	32.4
Condition II					
7	0.31–1.41	36.0	2	4.16	34.3
8	0.25–1.40	35.5	2	4.08	43.1
9	0.26–1.27	33.3	2	4.50	45.2
10	0.45–1.57	39.9	2	4.72	51.6
Condition III					
11	0.29–1.50	45.2	15	0.30	23.6
12	0.27–1.16	62.1	15	0.29	18.4
13	0.20–1.46	46.4	15	0.31	28.5
14	0.23–1.12	37.0	15	0.30	32.4
15	0.25–1.16	46.3	15	0.35	36.1
16	0.27–1.21	18.8	15	0.27	30.5
17	0.24–1.25	24.3	15	0.28	28.8
Condition IV					
18	0.24–1.24	31.5	15	3.61	38.2
19	0.30–1.23	26.4	15	3.93	43.1
20	0.33–1.48	38.8	15	3.90	35.0
21	0.26–1.28	35.4	15	4.19	45.8
22	0.32–1.40	48.2	15	4.00	27.8

[a] Pressure in the drift tube P_{dt} = 1.74 Torr, pressure in the flow tube P_{ft} = 100 Torr, electric field gradient E = 58.82 V cm^{-1}, E/N ratio = 104.4 Td, N is the concentration of the buffer gas. All the concentrations correspond to the initial values.

ton transfer reaction with H_3O^+ and were detected in their protonated forms by the mass spectrometry.

Seven products including both ring-retaining and ring-opening products were identified and quantified by ID-CIMS in this study. A product was verified on the basis of the molecular weight and mass spectra, by its response to varying OH and *m*-xyelne concentrations, and by a reasonable mechanistic deduction. All products identified in this study disappeared either when the microwave discharge was turned off or the flow of *m*-xylene was stopped, indicating that the products arisen from the OH-initiated oxidation of *m*-xylene. We were unable to discriminate the structural isomers solely on their mass spectra. Hence, some products were detected as the sum of all possible isomers. A mass spectral scan from m/z = 50 to 200 for the formation of the products of the OH–*m*-xylene reaction is shown in Fig. 2 for a typical experiment. *m*-xylene was the most prominent peak in the spectra (i.e. $C_8H_{11}^+$ or m/z = 107). Two ring-retaining products were identified as *m*-tolualdehyde ($C_8H_9O^+$ or m/z = 121) and *m*-dimethylphenols ($C_8H_{11}O^+$ or m/z = 123). Other peaks were attributed to the ring-opening carbonyl products. For example, the peaks at m/z = 73, 99, 113, 139, and 155 were identified as protonated methylglyoxal ($C_3H_5O_2^+$), unsaturated dicarbonyls (4-oxo-2-pentenal and 2-methyl-4-oxo-2-butenal, $C_5H_7O_2^+$), 4-oxo-2-methyl-2-pentenal ($C_6H_9O_2^+$), diunsaturated dicarbonyls (2-methyl-6-oxo-2,4-heptadienal and 4-methyl-6-oxo-2,4-heptadienal, $C_8H_{11}O_2^+$), and epoxy carbonyl isomers (2,4-dimethyl-2,3-epoxy-6-oxo-4-hexenal, 2,6-dimethyl-2,3-epoxy-6-oxo-4-hexenal, and 3,5-dimethyl-2-hydroxyl-3,4-epoxy-5-hexenal(ring-retaining), $C_8H_{11}O_3^+$), respectively, to be discussed in Section 4.

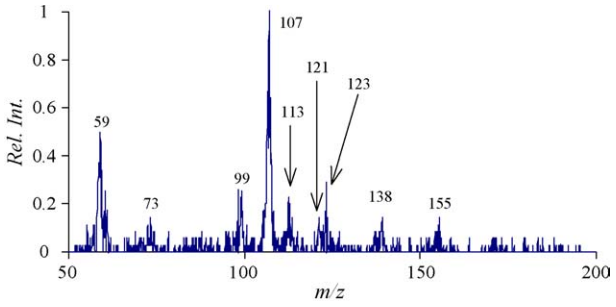

Fig. 2. Mass spectra for the OH-initiated oxidation of *m*-xylene using H_3O^+ as reagent ion under a typical experiment condition (e.g. experiment no. 15). Seven products were identified and quantified in the spectra.

As discussed in Section 2, by successively varying the *m*-xylene concentration, we quantified the product yields according to Eq. (5). For *m*-xylene, an ion–molecule rate constant of 2.26×10^{-9} cm^3 molecule^{-1} s^{-1} was taken from ref. [24]. For other products, we performed additional quantum chemical calculations to obtain their dipole moment and polarizability. The ion–molecule rate constants were determined using average-dipole orientation (ADO) theory. The rate constant of 1.90, 4.96, 4.27×10^{-9} cm^3 molecule^{-1} s^{-1} was used for methylglyoxal, 2-methyl-4-oxo-2-pentenal, and *m*-tolualdehyde, respectively. There were no substantial differences in the ion–molecule rate constants between the structural isomers. Hence, for a structural isomer, the rate constant used in this study was averaged over all possible isomers. The ion–molecule reaction rate constants were as follows (in 10^{-9} cm^3 molecule^{-1} s^{-1}): unsaturated dicarbonyls (4-oxo-2-pentenal and 2-methyl-4-oxo-2-butenal), 5.24; diunsaturated dicarbonyls (2-methyl-6-oxo-2,4-heptadienal and 4-methyl-6-oxo-2,4-heptadienal), 3.75; epoxy carbonyls (2,4-dimethyl-2,3-epoxy-6-oxo-4-hexenal, 2,6-dimethyl-2,3-epoxy-6-oxo-4-hexenal, and 3,5-dimethyl-2-hydroxyl-3,4-epoxy-5-hexenal), 5.06; and dimethylphenols (2,4- and 2,6-dimethylphenol), 2.96.

Plots of the amount of specific products formed against the amount of *m*-xylene reacted for typical experiments are shown in Fig. 3. The product yields were obtained from the slope of a linear least-square fit to the data. In contract to smog chamber experiments, reactions of the products with OH were neglected in this study because of the short residence time and small concentration of the products in the flow reactor. The major products from OH–*m*-xylene reaction were found to be methylglyoxal, its co-products (4-oxo-pentenal and 2-methyl-4-oxo-butenal), and dimehtylphenols. The yields (%) shown in Fig. 3 for the three products are 24.2, 21.9, and 18.2,

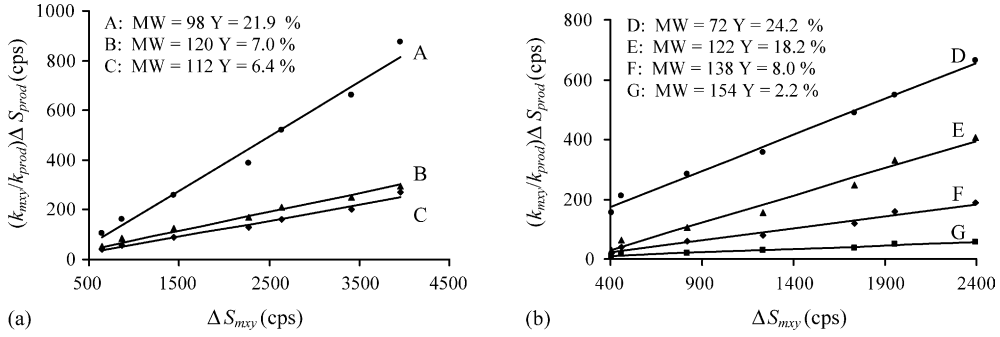

Fig. 3. Plots of the amount of the product formed against the amount of *m*-xylene reacted under the condition similar to those in experiment no. 18 (a) and no. 22 (b) in Table 1.

respectively. Other product yields shown in Fig. 3 are 6.4, 7.0, 8.0, and 2.2 for 2-methyl-4-oxo-2-pentenal, *m*-tolualdehyde, diunsaturated dicarbonyls, and epoxy carbonyls, respectively. Note that most lines fitted to the data (e.g. B, C, F and G in Fig. 3) extrapolated closely to the origin, while a few (e.g. A and E in Fig. 3) deviated from the origin, reflecting larger random errors for larger product yields due to data scattering. The line fitted to the data of methylglyoxal (D in Fig. 3) was found to possess the largest deviation, suggesting possible interference of methylglyoxal signal from the water clusters ($(H_2O)_4H^+$, $m/z = 73$).

The product distribution in this study was found to be dependent on the O_2 and NO concentrations. Table 2 lists the formation yields of the products (with 1σ error) under different experimental conditions. The uncertainty reflects both random errors due to data scattering as mentioned above and systematical errors (±25%) related to the ion–molecule rate constants and possible fragmentation of the products. For a fixed NO concentration, e.g. 0.3 ppm (under conditions I and III in Table 1), the yields increased with increasing O_2 concentration, from 10 to 15% for methylglyoxal and from 9.0 to 14.3% for unsaturated dicarbonyls (MW = 98), while the yield for dimethylphenols decreased from 25.0 to 17.3%. The yields for other products changed little considering the experimental errors. Similar observation was found for a fixed NO concentration of 4 ppm. Clearly, the bicylic radical channel is favorable under a higher concentration of O_2 (e.g. 15%), while at a lower concentration of O_2 (e.g. 2%) phenolic and oxide channels are favorable. For an O_2 mixing ratio of 2% (under conditions I and II in Table 1), the product yields were independent of the NO concentration. For example, the yields for *m*-tolualdehyde under conditions I and II were similar (6.99 and 8.65% under conditions I and II, respectively). Under conditions I and II, the formation yield of unsaturated dicarbonyls (4-oxo-pentenal and 2-methyl-4-oxo-butenal) was consistent with the estimated methylglyoxal yield (about 10%). For an O_2 mixing ratio of 15%, the product yields were independent of the NO concentration except for methylglyoxal and its co-products (4-oxo-pentenal and 2-methyl-4-oxo-butenal). The yields increased from 15 to 23% for methylglyoxal and from 14 to 20% for unsaturated dicarbonyls (4-oxo-pentenal and 2-methyl-4-oxo-butenal) with increasing NO concentrations from 0.3 to 4 ppm.

Although the NO_2 concentration was minimized, the secondary reaction of the OH–*m*-xylene adduct with NO_2 might not be completely ruled out. The rate constants of $(2–20) \times 10^{-16}$ cm^3 molecule^{-1} s^{-1} for the reactions of the OH–*m*-xylene and OH–*p*-xylene adducts with O_2 and 3×10^{-11} cm^3 molecule^{-1} s^{-1} for the reactions of the OH–*p*-xylene adduct with NO_2 have been measured [10–12]. Assuming the same rate constant for the reaction of the OH–*m*-xylene adduct with NO_2 as that of the OH–*p*-xylene adduct, the ratio of the reaction rates of the adduct with O_2 to

Table 2
Product formation yield (%) from OH-initiated oxidation of *m*-xylene in the presence of NO

Product	I[a]	II[a]	III[a]	IV[a]
Methylglyoxal (MW = 72)	∼10	∼10	15.1 ± 4.2	23.1 ± 5.0
Unsaturated dicarbonyls[b] (MW = 98)	8.99 ± 1.6	9.41 ± 2.2	14.3 ± 2.1	20.0 ± 7.1
2-Methyl-4-oxo-2-penetal (MW = 112)	3.26 ± 0.36	3.69 ± 0.50	4.89 ± 0.52	6.32 ± 1.5
m-Tolualdehyde (MW = 120)	6.99 ± 0.80	8.65 ± 0.95	6.42 ± 0.89	6.82 ± 1.16
m-Dimethylphenols[c] (MW = 122)	25.0 ± 5.3	22.3 ± 3.8	17.3 ± 2.5	15.2 ± 3.4
Diunsaturated dicarbonyls[d] (MW = 138)	10.1 ± 1.6	9.34 ± 1.4	7.82 ± 1.0	7.01 ± 1.6
Epoxy carbonyls[e] (MW = 154)	2.47 ± 0.32	2.89 ± 0.22	2.18 ± 0.20	2.21 ± 0.30

[a] See experimental conditions in Table 1.
[b] Sum of 4-oxo-2-pentenal and 2-methyl-4-oxo-2-butenal.
[c] Sum of 2,4-dimethylphenol and 2,6-dimethylphenol.
[d] Sum of 2-methyl-6-oxo-2,4-heptadienal and 4-methyl-6-oxo-2,4-heptadienal.
[e] Sum of 2,4-dimethyl-2,3-expoxy-6-oxo-4-hexenal, 2,6-dimethyl-2,3-expoxy-6-oxo-4-hexenal, and 3,5-dimethyl-2-hydroxyl-3,4-expoxy-5-hexenal.

NO_2 is about (0.7–7) $\times 10^{-5}$ $[O_2]/[NO_2]$, where $[O_2]/[NO_2]$ is the ratio of concentrations of O_2 to NO_2. Given a typical NO_2 concentration of ∼30 ppb in this study, the ratios are 5–50 and 38–380 for 2% (conditions I and II) and 15% (conditions III and IV) of O_2, respectively. Hence, with 2% of O_2 the reaction of OH–*m*-xylene adduct with NO_2 might not be negligible, while with 15% of O_2 the adduct reaction with NO_2 was unimportant. This likely explains the observed yield difference under different O_2 concentrations in this study. For an O_2 mixing ratio of 15%, the product yields resulting from the bicyclic pathway increased with the NO concentration, while yields of other products did not change appreciably with the NO concentration. This is anticipated considering the fact that NO is engaged in the bicyclic pathway, but is not involved in other channels of subsequent reactions after the addition of OH to *m*-xylene. The experimental condition III corresponds to the NO concentration in typical polluted air.

A comparison of the product yields quantified in this study with the literature values is summarized in Table 3. The methylglyoxal yield reported in this study (15%) is considerably lower than those reported (27–42%) previously [14,25–27]. A possible explanation for this discrepancy is that the secondary reactions of reactive dicarbonyl products could contribute substantially to the secondary formation of methylglyoxal reported by the smog chamber experiments, while secondary reactions in our study were negligible due to the short reaction time and low concentrations of the reactants. Note that both the short reaction time and low concentrations of the reactants are important factors to ensure negligible secondary reactions in our reaction system. The yield (14.3%) of the co-products of methylglyoxal, 4-oxo-2-pentenal, and 2-methyl-4-oxo-2-butenal, is consistent with the previous reports (12%, only for 4-oxo-2-pentenal) [14]. Also, the quantified yields of methylglyoxal and its co-products were very similar in our study. The consistency of the yield of methylglyoxal with that of its co-product is a strong signature of first generation species instead of secondary product for methylglyoxal. We were unable to quantify glyoxal because of substantial background interference from the peak at $m/z = 59$. This peak could be possible from a calibration comopound (perfluorotributylamine (PTA)) or oil originated from turbo pump. Alternatively, it could be from other unidentified sources. Several previous studies quantified the glyoxal yield, with a value of 8–13% (e.g. [28]). Three types of carbonyls have been identified but not been quantified previously, 2-methyl-4-oxo-2-pentenal, diunsaturated dicarbonyls, and epoxy carbonyls. We quantified these three products for the first time, with the yields of 4.9, 7.8, and 2.2%, respectively. The quantified yield of 2-methyl-4-oxo-2-pentenal (the co-product of glyoxal) would indicate that the yield of the first generation glyoxal could also be as low as 5%. A yield of 6.4% for *m*-tolualdehyde was determined in this study, consistent with a previous study [14]. The yield of dimethylphenols was within the range of the literature values [14,29].

Table 3
Comparison of product yields in this study with the previous measurements

Product	Yield (%)[a]	Reference
Glyoxal (MW = 58)	7.9 ± 0.4	[14]
	13 ± 3	[25]
	10.4 ± 2.0	[26]
	8.6 ± 1.1	[27,28]
Methylglyoxal (MW = 72)	40 ± 1.8	[14]
	42 ± 5	[26]
	26.5 ± 3.5	[25]
	31.9 ± 0.9	[27]
	15.1 ± 4.2	This work
Unsaturated dicarbonyls (MW = 98)	12 ± 1.2[b]	[14]
	14.3 ± 2.1	This work
2-Methyl-4-oxo-2-penetal (MW = 112)	4.89 ± 0.52	This work
m-Tolualdehyde (MW = 120)	4.85 ± 0.36	[14]
	6.42 ± 0.89	This work
m-Dimethylphenols (MW = 122)	10.9 ± 0.73[c]	[14]
	21.0	[29]
	17.3 ± 2.54	This work
Diunsaturated dicarbonyls (MW = 138)	7.82 ± 1.0	This work
Epoxy carbonyls (MW = 154)	2.18 ± 0.20	This work

[a] Yields reported in this work are under condition III.
[b] Only 4-oxo-penetal.
[c] Sum of 2,4-dimethylphenol, 2,6-dimethylphenol, and 3,5-dimethylphenol.

4. Reaction mechanisms

Formation of *m*-tolualdehyde from OH–*m*-xylene reaction has been well understood. As shown in Scheme 1, H-abstraction by OH from one methyl group of *m*-xylene leads to the formation of methylbenzyl radicals and subsequent addition of O_2 results in benzyl peroxy radicals. The peroxy radicals further react with NO to form alkoxy radicals and subsequent abstraction of alkoxy radicals by O_2 forms *m*-tolualdehyde. Under the different conditions used in this study, the measured yields were nearly invariant for *m*-xylene, suggesting *m*-tolualdehyde could be used as a reference compound for other products.

Carbonyl products in the ring-opening route have been suggested as an important radical source and have a large impact on ozone formation in the aromatic hydrocarbon oxidation [1–3]. Quantum chemical calculation showed that the addition of OH to *m*-xylene occurs predominately (greater than 90%) at the *ortho* position (J. Fan and R. Zhang, unpublished results). The bicyclic route is a major ring-opening product channel for OH–*m*-xylene system. Bicyclic radicals resulting from the primary peroxy radical form secondary peroxy radicals on addition of O_2 which then react with NO to form alkoxy radicals (Scheme 2). The alkoxy radicals can further decompose to form unsaturated dicarbonyls and corresponding α-hydroxyl radicals. Subsequent abstraction of α-hydroxyl radicals by O_2 results in the formation of glyoxal (J in Scheme 2) or methylglyoxal (I in Scheme 2).

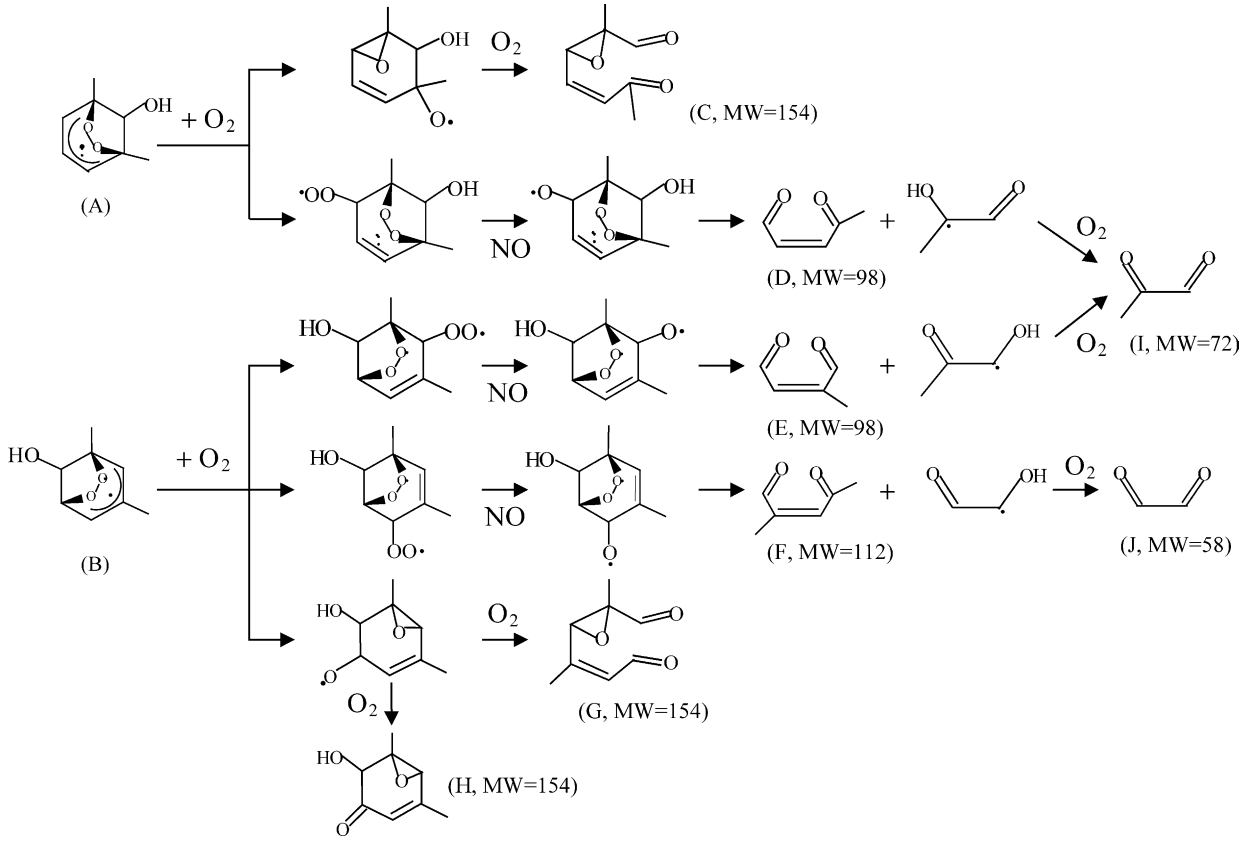

Scheme 2. Mechanistic diagram of the bicyclic pathway from OH-initiated oxidation of *m*-xylene.

Formation of 2-methyl-4-oxo-2-butenal (E in Scheme 2), 4-oxo-2-pentenal (D in Scheme 2), and 2-methyl-4-oxo-2-pentenal (F in Scheme 2) are depicted in Scheme 2, along with the glyoxal and methylglyoxal channels.

Diunsaturated dicarbonyls have been identified [17,30] but have not been quantified in previous studies because of the difficulty in experimental settings of the smog chamber experiments. These compounds undergo rapid photolysis or reaction with OH radicals. Quantification of the carbonyl product yields is advantageous using ID-CIMS in conjunction with a turbulent flow reactor in light of the short reaction time and low reactant concentrations. Several mechanisms were proposed for the formation of diunsaturated dicarbonyls from the OH-initiated oxidation of aromatic hydrocarbons. For OH–toluene reaction system, recent theoretical studies showed the primary peroxy pathway with NO to NO_2

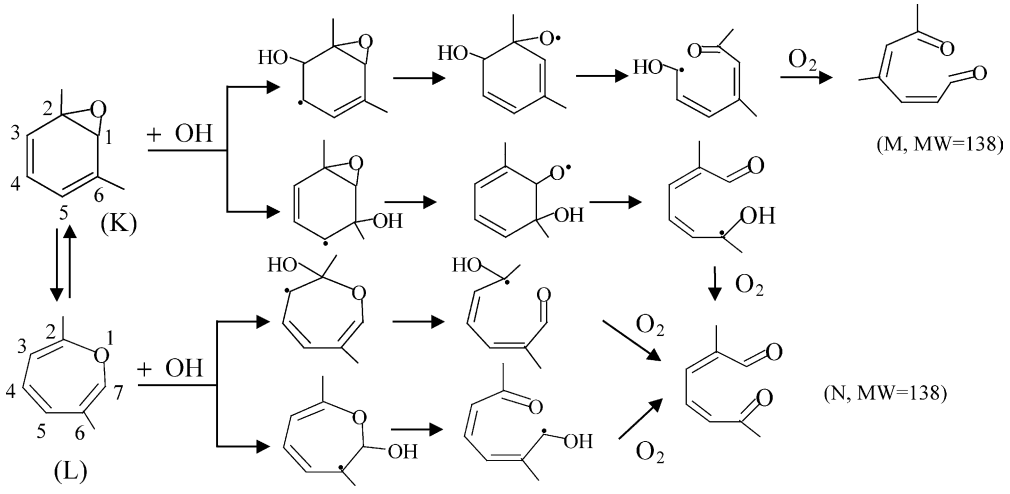

Scheme 3. Mechanistic diagram of the *m*-xylene-oxide/oxepin pathway from OH-initiated oxidation of *m*-xylene.

conversion to be implausible under atmospheric conditions [13,31]. Experimental observations provided evidence on an alternative route for the formation of diunsaturated dicarbonyls. For example, on the basis of the observed prompt HO_2 formation from the OH–toluene reaction system, Siese et al. proposed an abstraction pathway for the OH–toluene adduct by O_2, forming toluene oxides [32]. For the OH–*m*-xylene reaction, we estimated a first-order rate of about 10 and $10^2\ s^{-1}$ under NO concentrations of 0.3 and 3 ppm used in this study, respectively, assuming a rate constant on the order of $10^{-11}\ cm^3\ molecule^{-1}\ s^{-1}$ for the NO-peroxy radical reaction [1,2]. However, the estimated isomerization of the primary peroxy radical to bicyclic radical is on the order of $10^5\ s^{-1}$ (J. Fan and R. Zhang, unpublished results), significantly faster than the competing reaction with NO even with the high concentration of NO used in this study. Hence, 2-methyl-6-oxo-2,4- heptadienal and 4-methyl-6-oxo-2,4-heptadienal were most likely formed from the *m*-xylene-oxide/oxepin channel. As depicted in Scheme 3, following the formation of *m*-xylene-1,2-oxide (K in Scheme 3), a rapid equilibrium is established with its monocyclic isomer, 2,6-dimethyloxepin (L in Scheme 3). The aromatic-oxide/oxepin is fairly reactive toward OH radicals, with a reaction rate of $2 \times 10^{-10}\ cm^3\ molecule^{-1}\ s^{-1}$ for toluene-oxide with OH [33]. Addition of OH to C6 or C3 position (see Scheme 3) of *m*-xylene-1,2-oxide with two successive ring cleavages and then H-abstraction by O_2 leads to the formation of 2-methyl-6-oxo-2,4-heptadienal (N in Scheme 3) and 4-methyl-6-oxo-2,4-hexadienal (M in Scheme 3), respectively. Alternatively, addition of OH to C2 or C7 position of 2,6-dimethyloxepin, followed by ring fragmentation and H-abstraction, produces 2-methyl-6-oxo-2,4-heptadienal.

Epoxides have been considered for public health concern because of their carcinogenic and mutagenic properties. Bartolotti and Edney [34] suggested formation of epoxide intermediates from the OH-initiated oxidation of toluene in their theoretical studies. Epoxides have been identified as intermediates from atmospheric oxidation of aromatic compounds. Yu and Jeffries found experimental evidence for expoxides by detecting compounds with molecular weight matching a series of expoxides resulting from OH-initiated oxidation of a series of hydrocarbon [6]. For example, they identified 2,3-epoxy-2,4-dimethyl-6-oxo-4-heptenal as an intermediate from OH-initiated oxidation of 1,3,5-TMB. Quantification of epoxides was difficult in smog chamber experiments because of their low yield and high reactivity. In this study, we quantified epoxides using ID-CIMS technique. As discussed above, the bicyclic radicals resulting from the O_2 addition to the OH–*m*-xylene adduct react with O_2 to form secondary peroxy radicals. Alternatively, the bicyclic radicals undergo further intramolecular rearrangement to form epoxy alkoxy radicals. Subsequent fragmentation, then followed by H-abstraction results in the formation of two epoxy carbonyls: 2,6-dimethyl-2,3-epoxy-6-oxo-4-hexenal (C in Scheme 2), 2,4-dimethyl-2,3-epoxy-6-oxo-4-hexenal (G in Scheme 2). Alternatively, the epoxy alkoxy radicals directly lead to formation of a ring-retaining epoxy carbonyl (3,5-dimethyl-2-hydroxyl-3,4-epoxy-5-hexenal, H in Scheme 2) through H-abstraction by O_2.

5. Conclusions

A wide range of products from the OH-initiated oxidation of *m*-xylene in the presence of O_2 and NO have been identified and quantified using a turbulent flow reactor in conjunction with ID-CIMS detection. Products measured in this study account for about 47% of the carbon balance of *m*-xylene, compared with about 41% of *m*-xylene reported by Smith et al. [14]. Three carbonyl compounds resulting from the bicyclic route have been quantified for the first time. In the atmosphere, further oxidation of these carbonyls may contribute substantially to the formation of ozone. Among these carbonyl compounds, epoxides are of great interest in light of their toxic and mutagenic properties. The quantification of diunsaturated dicarbonyl compounds validates the aromatic-oxide/oxepin pathway and hence improves our understanding of aromatic hydrocarbon oxidation.

Acknowledgments

This work was supported by the Robert A. Welch Foundation (Grant A-1417) and the US Environmental Protection Agency EPA (R03-0132). The work was performed while K. Misawa was visiting Texas A&M University.

References

[1] J.G. Calvert, R. Atkinson, K.H. Becker, R.M. Kamens, J.H. Seinfeld, T.J. Wallington, G. Yarwood, The Mechanisms of Atmospheric Oxidation of Aromatic Hydrocarbons, Oxford University Press, New York, 2002.
[2] R. Atkinson, J. Phys. Chem. Ref. Data 26 (1997) 215–290.
[3] M.J. Molina, R. Zhang, K. Broekhuizen, W. Lei, R. Navarro, L.T. Molina, J. Am. Chem. Soc. 121 (10) (1999) 225–10226.
[4] J.R. Odum, T.P.W. Jungkamp, R.J. Griffin, R.C. Flagan, J.H. Seinfeld, Science 276 (1997) 96–99.
[5] H.J.L. Forstner, R.C. Flagan, J.H. Seinfeld, Environ. Sci. Technol. 31 (1997) 1345–1358.
[6] J. Yu, H.E. Jeffries, Atmos. Environ. 31 (1997) 2281–2287.
[7] R. Zhang, I. Suh, J. Zhao, D. Zhang, E.C. Fortner, X. Tie, L.T. Molina, M.J. Molina, Science 304 (2004) 1487–1490.
[8] W.P.L. Carter, Air Waste 44 (1994) 881–899.
[9] F. Kramp, S.E. Paulson, J. Phys. Chem. A 102 (1998) 2685–2690.
[10] R. Atkinson, J. Phys. Chem. Ref. Data Monogr. 2 (1994) 1–216.
[11] R. Knispel, R. Koch, M. Siese, C. Zetzsch, Ber. Bunsen-Ges. Phys. Chem. 94 (1990) 1375–1379.
[12] R. Koch, R. Knispel, M. Siese, C. Zetzsch, Absolute rate constants and products of secondary steps in the atmospheric degradation of aromatics, in: G. Angeletti, G. Restelli (Eds.), Proceedings of the Sixth European Symposium on the Physico-Chemical Behavior of Atmospheric Pollutants, European Commission, 1994, pp. 143–149.
[13] I. Suh, R. Zhang, L.T. Molina, M.J. Molina, J. Am. Chem. Soc. 115 (2003) 12655–12665.

[14] D.F. Smith, T.E. Kleindienst, C.D. McIver, J. Atmos. Chem. 34 (1999) 339–364.
[15] R. Volkamer, U. Platt, K. Wirtz, J. Phys. Chem. A 105 (2001) 7865–7874.
[16] H.L. Bethel, R. Atkinson, J. Arey, J. Phys. Chem. A 104 (2000) 8922–8929.
[17] E.S.C. Kwok, D.M. Aschmann, R. Atkinson, J. Arey, J. Chem. Soc., Farady Trans. 93 (1997) 2847–2854.
[18] E.C. Fortner, J. Zhao, R. Zhang, Anal. Chem. 76 (2004) 5436–5440.
[19] R. Zhang, I. Suh, W. Lei, A.D. Clinkenbeard, S.W. North, J. Geophys. Res. 105 (2000) 24627–24635.
[20] W.B. DeMore, S.P. Sander, C.J. Howard, A.R. Ravishankara, D.M. Golden, D.E. Kolb, R.F. Hampson, M.J. Kurylo, M.J. Molina, Chemical Kinetics and Photochemical Data for Use in Stratospheric Modeling, NASA, Jet Propulsion Laboratory, Pasadena, CA, 1997 (JPL publication 97-4).
[21] D. Zhang, R. Zhang, C. Church, S.W. North, Chem. Phys. Lett. 343 (2001) 49–54.
[22] D. Zhang, R. Zhang, S.W. North, J. Phys. Chem. 107 (2003) 11013–11019.
[23] J. Zhao, E.C. Fortner, R. Zhang, J. Am. Chem. Soc. 126 (2004) 2686–2687.
[24] J. Zhao, R. Zhang, Atmos. Environ. 38 (2004) 2177–2185.
[25] H. Bandow, N. Washida, Bull. Chem. Soc. Jpn. 58 (1985) 2541–2548.
[26] E.C. Tuazon, R. Atkinson, H. MacLeod, H.W. Biermann, A.M. Winer, W.P.L. Carter, J.N. Pitts, Environ. Sci. Technol. 18 (1984) 981–984.
[27] E.C. Tuazon, H. MacLeod, R. Atkinson, W.P.L. Carter, Environ. Sci. Technol. 20 (1986) 383–387.
[28] M. Gery, D. Fox, R. Kamens, L. Stockburger, Environ. Sci. Technol. 21 (1987) 339–348.
[29] R. Atkinson, S. Aschmann, J. Arey, Int. J. Chem. Kinet. 23 (1991) 77–97.
[30] J. Yu, H.E. Jeffries, Atmos. Environ. 31 (1997) 2261–2280.
[31] I. Suh, D. Zhang, R. Zhang, L.T. Molina, M.J. Molina, Chem. Phys. Lett. 364 (2002) 454–462.
[32] M. Siese, R. Koch, C. Fittchen, C. Zetzsch, in: P.M. Borell, P. Borell, T. Cvitas, W. Seiler (Eds.), Transport and Transformation of Pollutants in the Troposphere, Academic Publishing, The Hague, Netherlands, 1994, pp. 115–118.
[33] B. Klotz, I. Barnes, B.T. Golding, K.-H. Becker, Phys. Chem. Chem. Phys. 2 (2000) 227–235.
[34] L.J. Bartolotti, E.O. Edney, Chem. Phys. Lett. 245 (1995) 119–122.